Density functional study of the magnetic properties of Bi_4Mn clusters: Discrepancy between theory and experiment

J. Botana, M. Pereiro, D. Baldomir, and J. E. Arias

Citation: J. Chem. Phys. **134**, 034307 (2011); doi: 10.1063/1.3521270

View online: https://doi.org/10.1063/1.3521270

View Table of Contents: http://aip.scitation.org/toc/jcp/134/3

Published by the American Institute of Physics

Density functional study of the magnetic properties of Bi_4Mn clusters: Discrepancy between theory and experiment

J. Botana,[1,2,a)] M. Pereiro,[1,2] D. Baldomir,[1,2] and J. E. Arias[2]
[1]*Dpto. Física Aplicada, Facultade de Física, Universidade Santiago de Compostela, E-15782 Santiago de Compostela, Spain*
[2]*Instituto de Investigacións Tecnolóxicas, Universidade de Santiago de Compostela, E-15782 Santiago de Compostela, Spain*

(Received 9 July 2010; accepted 6 November 2010; published online 20 January 2011)

We have performed collinear and noncollinear calculations on neutral Bi_4Mn and collinear ones on ionized Bi_4Mn with charges $+1$ and -1 to find out why theoretical calculations will not predict the magnetic state found in the experiment. We have used the density functional theory to find a fit between the theoretical prediction of the magnetic moment and the experimental value. Our calculations have consisted in a structural search of local energy minima, and the lowest energy magnetic state for each resulting isomer. The geometry optimization found three local minima whose fundamental state is the doublet spin state. These isomers could not be found in previous theoretical works, but they are higher in energy than the lowest-lying isomer by ≈ 1.75 eV. This magnetic state could help understand the experiment. Calculations of noncollinear magnetic states for the Bi_4Mn do not lower the total magnetic moment. We conclude arguing how the three isomers with doublet state could actually be the ones measured in the experiment. © *2011 American Institute of Physics*. [doi:10.1063/1.3521270]

I. INTRODUCTION

Nanostructured materials have become the main source in current technology to develop devices with novel properties: atoms in low dimensional structures behave differently than as a part of bulk matter. Among them, the zero-dimensional materials, i.e., atomic clusters and nanoparticles, have attracted a great deal of attention, especially for their magnetism. Atoms in pure small clusters can exhibit far larger magnetic moments than when isolated or within crystals.[1–3] This effect can be enhanced when impurities are added.[4] In this trend, the study of transition metal binary clusters was triggered by the exceptionally high magnetism found in CoRh nanoparticles by Zitoun *et al.*[5] Since then, a number of magnetically enhanced nanoalloys of ferromagnetic and nonmagnetic transition metals have been studied theoretically[6–9] and experimentally.[10–12] Yin *et al.*[13] found an enhanced magnetism in BiMn clusters for Bi-to-Mn ratios close to 2 in their Stern–Gerlach measurements, which deviated from the trend in other Bi nanoalloys like BiCo, where the magnetic moment had a small dependence with cluster size.[10] In a later paper, Chen *et al.*[14] performed extensive density functional theory (DFT) calculations on Bi_nMn_m ($n = 1$–6, $m = 1$–12) clusters to learn their structure and how their magnetism works. While they have found quite a good agreement with the experiment for this series, there are a few large discrepancies between the theoretical value of the magnetic moment and the measured one. The most significative one is the Bi_4Mn where DFT calculations predict a total magnetic moment $\mu_T = 5\ \mu_B$ while the experiment measures $1.6\ \mu_B$. The cause of this discrepancy was not found, although extensive geometric optimizations and an estimation of the orbital contribution to the magnetic moment were performed to solve this problem.

In the present paper we will explore the possible sources of the mismatch between theoretical calculations and experimental results for the Bi_4Mn nanoalloy, through DFT calculations. We considered the following possibilities: finding isomers of the cluster whose total magnetic moment is low enough; allowing noncollinear magnetic states for the studied Bi_4Mn structures, as this might lower their magnetic moment; and finding out the orbital contribution to the magnetic moment of each structure. The paper is organized as follows: In Sec. II, we explain the computational methods we have used, also reasoning why each method was used seeking which result. In Sec. III, we show our results and discuss them, and it is divided in two subsections: Subsection III A contains the results of the calculations with imposed collinear magnetic moments, and subsection III B, the results of the calculations where the collinear constraint is lifted, allowing magnetic moments to arrange freely. Section IV contains the conclusions derived from our findings.

II. COMPUTATIONAL DETAILS

Our first step was to perform *ab initio* calculations within the framework of the DFT over a large number of different structures of Bi_4Mn, both taken from the literature and created by the authors. We solved each system using linear combinations of Gaussian-type orbitals within the Kohn–Sham (KS) density functional methodology (LCGTO-KSDFM), with the deMon 2003 code.[15] The calculation of the exchange-correlation (XC) energy term was carried out using the generalized gradient approximation (GGA), in the Perdew–Burke–Ernzerhof (PBE) ansatz.[16] It has been shown

a)Electronic mail: jorge.botana@usc.es.

that the GGA is the approximation that gives the best results for geometry optimizations of small clusters.[17,18] The orbital basis set used in our calculations[19] for Bi and Mn takes the Stuttgart–Dresden effective core potentials RECP|SD.[20] They explicitly consider the outer 15 electrons of the Mn using a relativistic approximation, and the outer five ones of the Bi with a quasirelativistic one. Spin-orbit coupling (SOC) is not considered in either case. While the SOC term is not negligible in Bi atoms, it has been reported not to have effects in the determination of the geometry of the ground state of their clusters, such as the Bi_4.[21] The electron density is expanded in auxiliary basis sets in order to avoid the calculation of the N^4 scaling Coulomb repulsion energy, where N is the number of the basis functions. The auxiliary basis sets are GEN-A3* (Ref. 22) for the Bi and A2-DZVP (Ref. 23) for Mn. The inner electrons of the atoms are represented with a core model, using the Hartwigsen–Goedecker–Hutter pseudopotentials.[24]

Each structure was geometrically optimized through a Born–Oppenheimer molecular dynamics simulation. After this first approach, the geometry of each cluster was optimized further with a Broyden–Fletcher–Goldfarb–Shanno algorithm.[25] Consecutively, we carried out a search in the collinear magnetic state that yields the energy minimum for zero external magnetic field and $T = 0$ for each geometry. The calculations were converged using 10^{-7} as the convergence criterion for the self-consistent cycle and 10^{-4} for the geometry optimization steps. It is worth noting that after this optimization, the initial structures to which we impose the different magnetic states often relax to different final structures, while different initial structures might converge to the same final structure. Hence, we obtain a large number of relaxed isomers, all of them local minima in their magnetic state. We focus on the 21 geometries with lower energy, performing single-point calculations for each isomer, searching for their fundamental magnetic state. The partial charges and magnetic moments for each one of the atoms are known through a Mulliken population analysis of the electrons. Next, we perform noncollinear single-point calculations to determine the lowest-energy magnetic state for each one of the 21 isomers. These calculations are performed using a different DFT implementation, the Octopus code.[26] The Octopus calculations consider wavefunctions to be complex spinors and they include the SOC relativistic correction. In the same manner as the collinear calculations, XC energy is approximated through a GGA-PBE functional. As for the grid upon which the KS equations are solved, we have chosen a radius of 4.4 Å and a spacing of 0.1 Å. The mixing scheme is a broyden one, with a mixing factor of 0.02. The convergence factor used was ConvRelDens $= 10^{-5}$.

III. RESULTS

A. Collinear calculation results

In Fig. 1 we represent the 21 lowest-energy isomers that we have found in our calculations and in Fig. 2 we plot the energies of each of their available magnetic states from 1 to 9 μ_B. Our lowest energy structure is an edge-capped distorted tetrahedron with $\mu_{\text{total}} = 5\ \mu_{\text{B}}$. This result agrees with Chen's

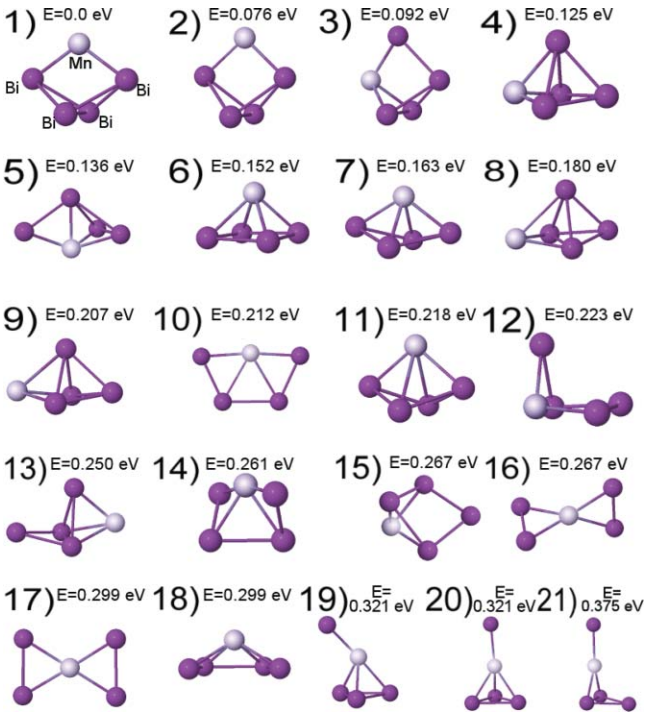

FIG. 1. Geometry of the 21 lowest-energy structures for the nanoalloy Bi_4Mn, with their relative energies per atom, in electron volts.

work[14] and is concurrently in disagreement with the experimental data.[13] In addition, our calculations over the two alternative geometries considered in Ref. 14, a pyramid and a W-like structures, are in good agreement with said work (see Fig. 2): the pyramidal structure (isomer 6 in Fig. 1) is 0.76 eV higher than the lowest-lying isomer, and the W-like structure (isomer 10 in Fig. 1) 1.06 eV higher.

The structures with $\mu_{\text{total}} = 5\ \mu_{\text{B}}$ dominate the lowest energy isomers until the 11th one, and from that point on, structures with $\mu_{\text{total}} = 3\ \mu_B$ dominate instead until the 18th one. Our three highest energy isomers have $\mu_{\text{total}} = 1\ \mu_B$, this being the μ_{total} closest to the experimental value of 1.6 μ_B.

Analyzing each atom of the nanoalloy separately, most of the magnetic moment comes from the Mn atom, while the Bi ones typically remain close to zero. As we can see in Fig. 3(a), electrons are shared from the Bi to the Mn, in particular from $6p$ orbitals to $4d$. This charge transfer does not generally enhance magnetism in either element, as the Mn total magnetic moment oscillates between 4 and 5 μ_B for all clusters, without correlation to charge transfers [see Fig. 3(b)]. In the three higher energy isomers, however, one of the Bi atoms stands isolated, bound only to the central Mn. This Bi, in addition to transferring $6p$ electrons to the Mn, also receives charge into its $7p$ orbital, greatly increasing its magnetic moment which couples antiparallel with the Mn. This makes the total magnetic moment of the isomer to decrease to 1 μ_B. The lower total magnetic moment state is hence originated in the enhancement of the magnetism of the Bi atoms, whose magnetic moments are either very close to zero or antiparallely aligned to those of the Mn atoms.

We have not found the lowest energy isomer to have a total magnetic moment close to the experimental value. Instead,

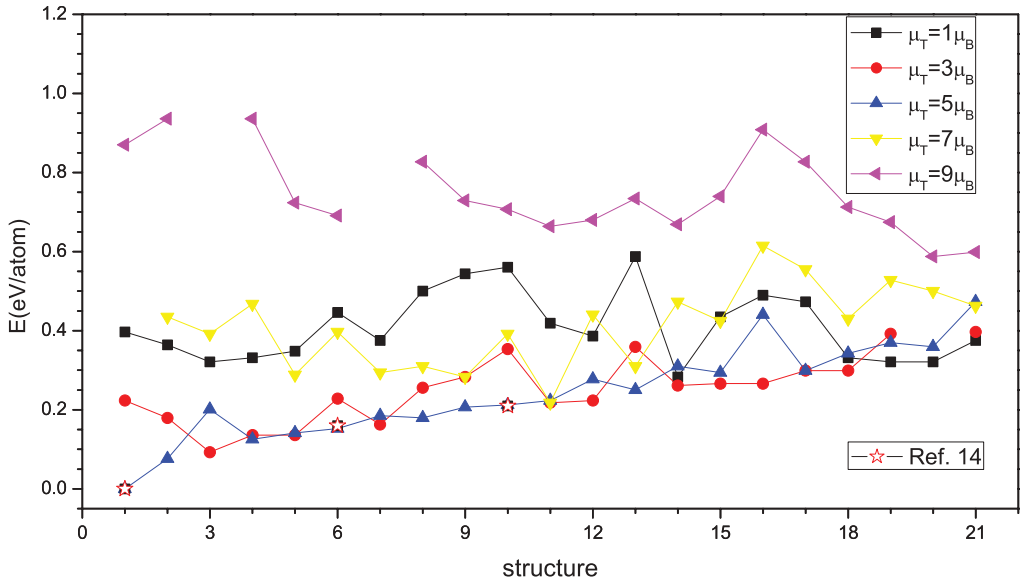

FIG. 2. Energy of the 21 structures with lower energy for the magnetic configurations $\mu_{\text{total}} = 1, 3, 5, 7, 9\ \mu_B$. The numbers in the x-axis correspond to the structures shown in Fig. 1. For the sake of comparison, we have included the relative energies to the lowest-lying isomer for the structures calculated by Chen *et al.* (Ref. 14).

the isomers with $\mu_T = 1$ (the ones closest to the experimental value) have a much higher energy than the ground state; hence, they could not make up a significative fraction of the experimental sample of Bi_4Mn.

We proceed to test other exchange-correlation functionals to find out if this could be the reason for the discrepancy. In Fig. 4, we show the ground states calculated for the lowest-lying isomer for different XC functionals, and we compare them with our results for PBE functional. We performed this calculation for the values of $\mu_T = 1, 3, 5\ \mu_B$. Local functionals exhibit higher energies, but all functionals provide the same energetic ordering of the three magnetic states: $\mu_T = 5\ \mu_B$ as the lowest, $3\ \mu_B$ second lower, and $1\ \mu_B$ third lower. When splitting the energy in XC and classical terms, all the considered functionals keep the same ordering: XC term greatly favors the $3\ \mu_B$ and $5\ \mu_B$ states, while the bias

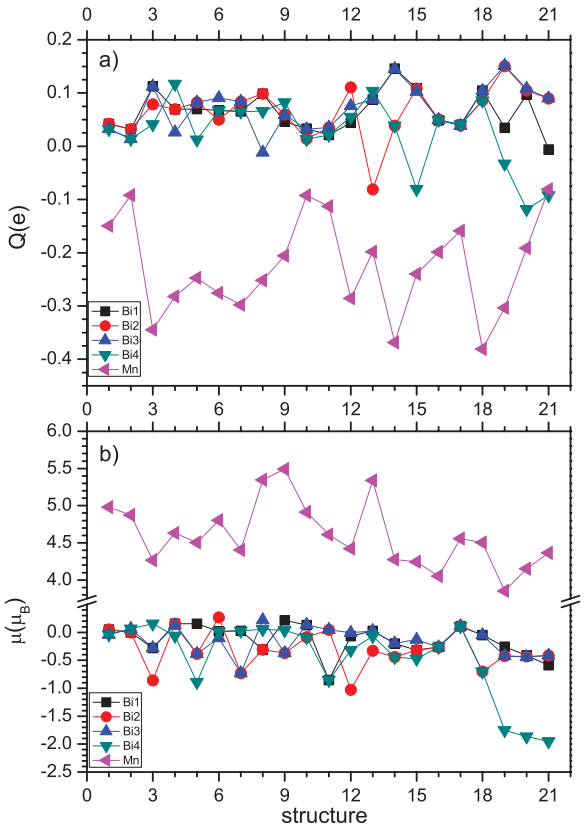

FIG. 3. Atomic charges (a) and magnetic moments (b) of each atom in the ground state of each one of the 21 lowest energy isomers of Bi_4Mn.

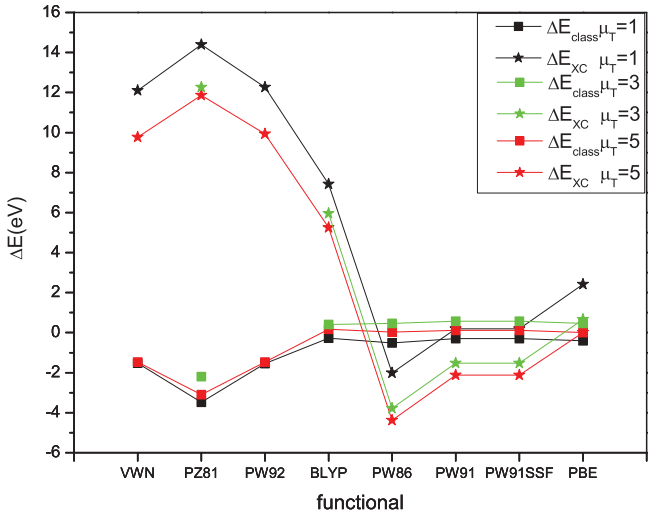

FIG. 4. Comparison of the three lowest magnetic states of the lowest-lying isomer of Bi_4Mn calculated using different XC functionals. VWN is a Dirac exchange (Ref. 27) with local VWN correlation (Ref. 28) PZ81, Dirac exchange with local PZ81 correlation (Ref. 29) PW92, Dirac exchange with local PW92 correlation (Ref. 30). BLYP, B88 GGA exchange (Ref. 31) with LYP GGA correlation (Ref. 32). PW86, PW86 GGA exchange (Ref. 33) with P86 GGA correlation (Ref. 34). PW91, PW91 GGA exchange and correlation (Ref. 35). PW91SSF, PW91 with full spin scaling function. PBE, PBE GGA exchange and correlation (Ref. 16).

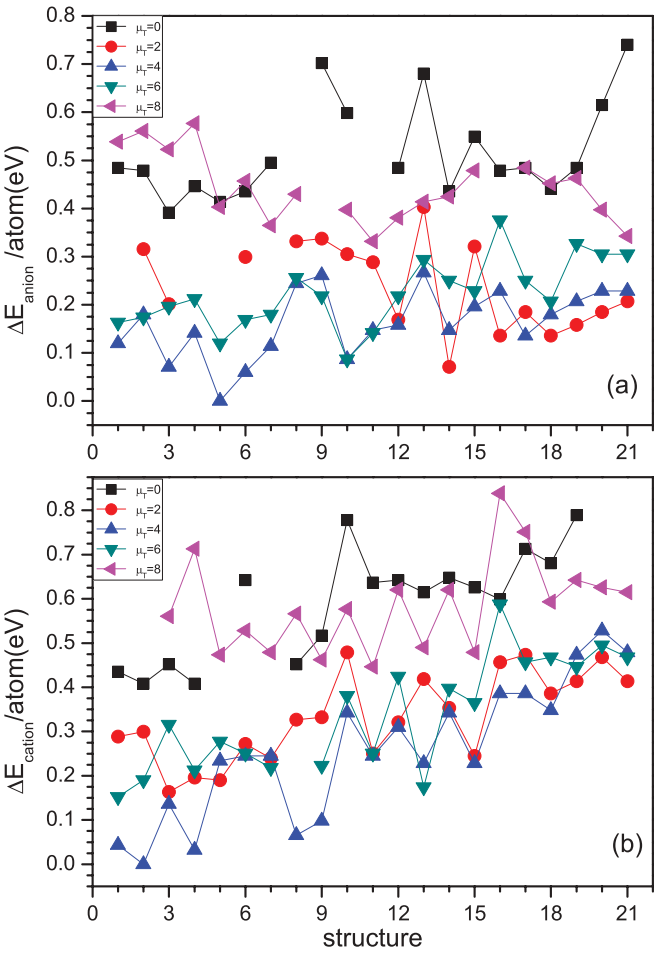

FIG. 5. Energy comparison of the 21 structures with lower energy for the magnetic configurations $\mu_T = 0, 2, 4, 6, 8\ \mu_B$ of the negatively (a) and positively (b) charged ions of Bi_4Mn.

of the classical term lowering the 1 μ_B state cannot balance it.

The final scenario we can examine with collinear calculations is the possible ionization of the experimental BiMn clusters during their production, or that their structure changes during the ionization in the Stern–Gerlach experiment. This is unlikely because of the low temperature of the process.[36] The results still do not yield any significative reduction of the total magnetic moment, as we can see in Fig. 5. The lowest-lying isomers are small deformations of the one for the neutral cluster, and the lowest magnetic configuration is 4 μ_B both for positive and negative ions. The lowest magnetic state of the anions is found for their third lowest-lying isomer, which has $\mu_T = 2\ \mu_B$. Even this result is larger than the experimental value, so it cannot explain the discrepancy.

As a summary, we have found that there are three structures of the Bi_4Mn cluster whose $\mu_T = 1\ \mu_B$. The experimental value is 1.6 μ_B, which implies that it is not isomerically pure: there has to be a population mixture of clusters with different structures and different μ_T, including 1 μ_B. However, these three structures are ≈ 1.75 eV higher than the lowest-lying one, and there are 18 structures with lower energy than them. Consequently, it is unlikely that the experimental device can produce these isomers in a high enough ratio as to lower the magnetic moment, explaining the experimental value. Except that some other reason, unaccounted for in our calculations, happens to favour their synthesis. Nevertheless, there is another possible explanation for a fractional value of μ_T: that the magnetic moments of the cluster are not alligned collinearly. To explore this possibility, we proceeded to perform noncollinear calculations, where the magnetic moments are not constrained to match a single axis.

B. Noncollinear calculation results

The next step is to find out if the discrepancy can be solved with noncollinear calculations, performing them for the 21 lowest-energy structures we found in the collinear ones. As we can see in Fig. 6(a), the energy dependence of the different isomers with noncollinear magnetic configuration roughly follows that of the isomers with collinear magnetism. The total magnetic moment [see Fig. 6(b)] ranges from 3.7 to 6.4 μ_B, with the lowest-lying isomer having $\mu_T = 5.0\ \mu_B$, values which agree with the collinear calculations for the lowest energy clusters, exceeding the experimental result. The ratio of the moduli of the total magnetic moment components: M_x and M_y against M_z is very small, specially for the lower energy isomers. We can conclude that the collinear approximation is a good one, which validates the results of our collinear calculations in subsection III A.

Further analysis of the magnetic components of our isomers yield the orbital magnetic moment: in Fig. 6(c), we compare the modulus of the orbital magnetic moment with the value for BiMn in bulk, 0.17 μ_B,[37] seeing that the value of the orbital magnetic moment has the same order of magnitude, being small in all cases. Studying the orbital component and comparing it with the total magnetic moment of each isomer, we find that in all cases this contribution is smaller than 10%, except for the structure 16, where the ratio between the moduli is 14%. From our results, we conclude that the orbital magnetic moment for these clusters is too small to be a significative factor in the total magnetic moment, so it cannot be the source of the discrepancy between the experimental results and the theoretical calculations. Furthermore, our calculated orbital magnetic moments for each isomer are well within the upper limit estimated by Chen *et al.*, $1.35\mu_B$.

IV. CONCLUSIONS

We have explored the possible scenarios that could lead to the known discrepancy between the experimental value of the total magnetic moment of the Bi_4Mn cluster and the theoretically calculated one. We have found that three isomers among the 21 most stable actually have a total magnetic moment below the experimental one, but these isomers are too high in energy respect to the lowest-lying one. Furthermore, there are 18 isomers with lower energy, so these three cannot make up for a fraction of the population of randomly created Bi_4Mn clusters significative enough to reduce the

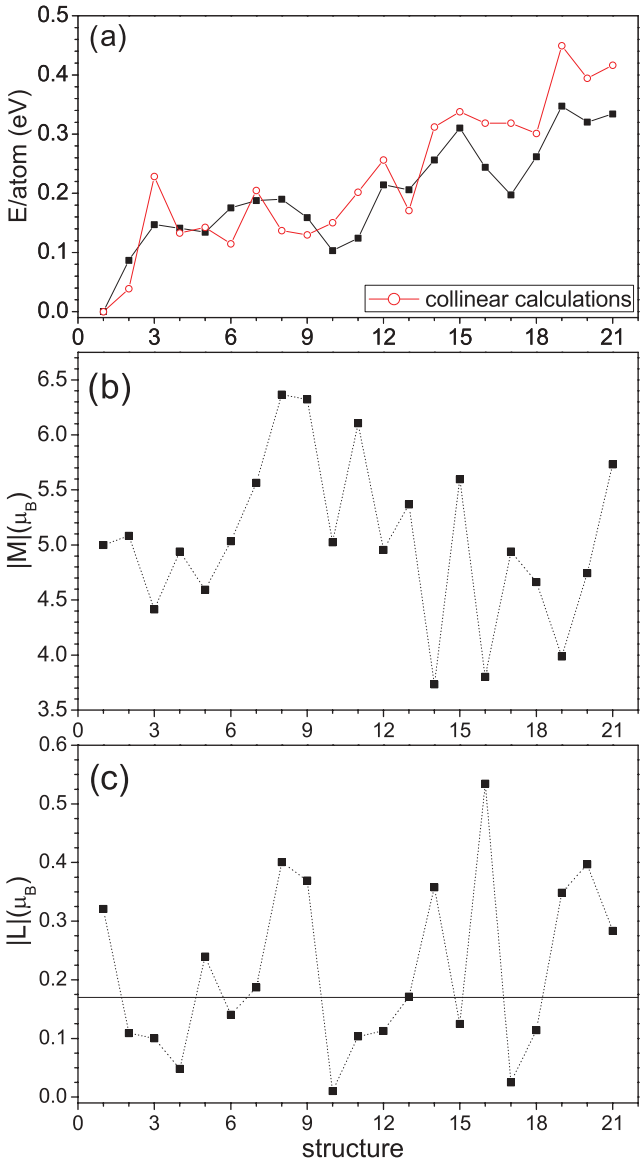

FIG. 6. Energy (a), magnetic moments (b), and orbital moments (c) for the 21 lowest-energy isomers of Bi_4Mn found in the noncollinear calculations. In (a) we have included the energies of the different isomers from collinear calculations using the Octopus code, for comparison. In (c), the horizontal line marks the value of the orbital magnetic moment in bulk BiMn.

average total magnetic moment down to the experimental value. We have found that any of the used XC functional approximations does not make the ground state of the lowest-lying isomer have a lower magnetic moment. The analysis of the positive and negative singly charged ions has also yielded no lowest-energy structure with a magnetic moment close to the experimental one. In fact, none of the ions of the 21 isomers we have considered has a ground state with a magnetic moment lower than the experiment. This should be expected though, as the only lower magnetic state available to ions of Bi_4Mn is a singlet. The possible presence of ions would not help us explain the experiment unless we had found ground states at $\mu_T = 0\ \mu_B$. From our noncollinear calculation, we rule out other two possible sources of the disagreement: (i) the magnetic configuration is collinear to a high degree, even when allowing the individual atomic magnetic moment to arrange freely, and still produces states with high magnetic moment: between 4 and 6.4 μ_B, hence this cannot be the source. (ii) The orbital magnetic moment is too low in absolute value compared to the total magnetic moment to produce a significant reduction in it.

All these consistently negative results in our search for a source of the discrepancy in the calculations suggest that said source is not an actual error of the calculations. Furthermore, the possibility that DFT method itself is not reliable to study this cluster is unlikely: the DFT results are in fairly good agreement for almost all the other Bi_mMn_n clusters. Having this in account, we are only left with the explanation suggested in subsection III A, i.e., that the experimental sample of Bi_4Mn is composed of a population of different structures and that one or some of our structures 19, 20, 21 are a significative fraction of said sample. We have found no reason why DFT would increase the energy of these structures specifically, so there could be a factor in the experiment that favors their production. We think it is remarkable that the structures 19, 20, 21 are very similar the lowest-lying isomer for Bi_3Mn clusters (a tetrahedron), simply adding an extra Bi atom to the Mn end of the tetrahedron. If Bi_3Mn clusters form much more quickly in the experimental device than Bi_4Mn ones, it is not unreasonable to think that the later will form from the former. Bi_3Mn also has a large electrostatic dipole we have calculated to be 2.4 D in the direction that connects the Mn atom with the center of the triangle formed by the three Bi atoms. This dipolar moment could help a fourth Bi atom to couple to the Mn instead of breaking up the tetrahedron to form the calculated Bi_4Mn lowest-lying structure. If the process of measurement of mass and magnetic moment of the clusters is fast enough, they might not have enough time to relax into the said lowest-lying isomer, hence resulting in some of our structures 19, 20, or 21 making up a large fraction of the measured Bi_4Mn clusters.

To verify this, one possible path would be to perform an analysis of the optical properties of the experimentally obtained Bi_4Mn clusters to identify their geometry, and see if they match with the isomers theoretically obtained as the lowest energy ones, or instead they match with any of the 19, 20, 21 isomers that actually show a low total magnetic moment. If the later case were true, then we would have to explain why the experimental setup produces structures that theoretically at T = 0 K are known not to be the fundamental one. On the other case, it would be necessary to know why the theory cannot predict the correct magnetic moment for a cluster with known composition and structure. The flight-time of the experimentally obtained clusters through the Stern–Gerlach device is 10 ms, but at this moment we do not have the means to estimate the time it takes a cluster to relax to the lowest-lying structure. Time-dependent DFT or quantum mechanical-molecular mechanics calculations should be the following step to introduce both the time coordinate and nonzero temperatures, and estimate the estructural relaxation time, to compare it with the experimental flight-time. In addition, regular DFT calculations could be improved by use of optimized-effective-potential method instead of XC functionals.

ACKNOWLEDGMENTS

We wish to acknowledge the Centro de Supercomputación de Galicia (CESGA) for the computing resources and the advice they have made available for us. We would like to thank Dr. Pardo for helpful discussions. This research has been done under the Projects No. MAT2009-08165 and No. INCITE08PXIB236052PR. One of the authors has been enjoying financial support from the Isabel Barreto program.

[1] I. M. L. Billas, A. Chatelain, and W. A. de Heer, Science **265**, 1682 (1994).
[2] J. A. Alonso, Chem. Rev. **100**, 637 (2000).
[3] M. Pereiro, D. Baldomir, and J. E. Ariasi, Phys. Rev. A **75**, 063204 (2007).
[4] S.-Y. Wang, J.-Z. Yu, H. Mizuseki, Q. Sun, C.-Y. Wang, and Y. Kawazoe, Phys. Rev. B **70**, 165413 (2004).
[5] D. Zitoun, M. Respaud, M.-C. Fromen, M. J. Casanove, P. Lecante, C. Amiens, and B. Chaudret, Phys. Rev. Lett. **89**, 037203 (2002).
[6] E. O. Berlanga-Ramírez, F. Aguilera-Granja, J. M. Montejano-Carrizales, A. Diaz-Ortiz, K. Michaelian, and A. Vega, Phys. Rev. B **70**, 014410 (2004).
[7] H. Y. Kim, H. G. Kim, J. H. Ryu, and H. M. Lee, Phys. Rev. B **75**, 212105 (2007).
[8] T. Sondón, J. Guevara, and A. Saúl, Phys. Rev. B **75**, 104426 (2007).
[9] M. Pereiro, D. Baldomir, and J. E. Arias, Phys. Rev. B **80**, 075412 (2009).
[10] T. Hihara, S. Pokrant, and J. A. Becker, Chem. Phys. Lett. **294**, 357 (1998).
[11] S. Pokrant and J. A. Becker, J. Magn. Magn. Mater. **226–230**, 1921 (2001).
[12] S. Yin, R. Moro, X. Xu, and W. A. de Heer, Phys. Rev. Lett. **98**, 113401 (2007).
[13] S. Yin, X. Xu, R. Moro, and W. A. de Heer, Phys. Rev. B **72**, 174410 (2005).
[14] H. Chen, H. K. Yuan, A. L. Kuang, Y. Miao, P. Chen, and Z. H. Xiong, Phys. Rev. B **77**, 184429 (2008).
[15] A. M. Koester, R. Flores-Moreno, G. Geudtner, A. Goursot, T. Heine, J. U. Reveles, A. Vela, and D. R. Salahub, *deMon 2003 code* (NRC, Canada, 2003)
[16] J. P. Perdew, K. Burke, and M. Ernzerhof, Phys. Rev. Lett. **77**, 3865 (1996).
[17] M. Pereiro, D. Baldomir, M. Iglesias, C. Rosales, and M. Castro, Int. J. Quantum Chem. **81**, 422 (2001).
[18] K. Yabana and G. F. Bertsch, Phys. Rev. A **60**, 3809 (1999).
[19] S. Huzinaga, J. Andzelm, M. Kłbukowski, E. Radzio-Andzelm, Y. Sakai, and H. Tatewaki, *Gaussian Basis Sets for Molecular Calculations* (Elsevier, Amsterdam, 1984).
[20] www.theochem.uni-stuttgart.de/pseudopotentials, 20.02.03, R. Flores-Moreno.
[21] H. Zhang and K. Balasubramanian, J. Chem. Phys. **97**, 3437 (1997).
[22] A. M. Koester, P. Calaminici, S. Escalante, R. Flores-Moreno, A. Goursot, S. Patchkovskii, J. U. Reveles, D. R. Salahub, A. Vela, and T. Heine, *The deMon User's Guide, Version 1.0.3* (Elsevier, 2003-2004), Appendix A.
[23] A. M. Koester, R. Flores-Moreno, G. Geudtner, A. Goursot, T. Heine, J. U. Reveles, A. Vela, and D. R. Salahub, *deMon 2003 code* (NRC, Canada, 2003), creation (29-03-96, A. M. Koester and M. Krack).
[24] C. Hartwigsen, S. Goedecker, and J. Hutter, Phys. Rev. B **58**, 3641 (1998).
[25] H. B. Schlegel, *Modern Electronic Structure Theory* (Word Scientific, Singapore, 1995), p. 495.
[26] M. A. L. Marques, A. Castro, G. F. Bertsch, and A. Rubio, Comput Phys. Comm. **151**, 60 (2003).
[27] P. A. M. Dirac, Proc. Cambridge Philos Soc. **26**, 376 (1930).
[28] S. H. Vosko, L. Wilk, and M. Nusair, Can. J. Phys. **58**, 1200 (1980).
[29] J. P. Perdew and A. Zunger, Phys. Rev. B **23**, 5048 (1981).
[30] J. P. Perdew and Y. Wang, Phys. Rev. B **45**, 13244 (1992).
[31] A. D. Becke, Phys. Rev. A **38**, 3098 (1988).
[32] C. Lee, W. Yang, and R. G. Parr, Phys. Rev. B **37**, 785 (1988).
[33] J. P. Perdew and Y. Wang, Phys. Rev. B **33**, 8800 (1986).
[34] B. Zimmermann, Ph.D. thesis, Universistat Hannover, (1999).
[35] J. P. Perdew, J. A. Chevary, S. H. Vosko, K. A. Jackson, M. R. Pederson, D. J. Singh, and C. Fiolhais, Phys. Rev. B **46**, 6671 (1992).
[36] R. Moro, S. Yin, X. Xu, and W. A. de Heer, Phys. Rev. Lett. **93**, 086803 (2004).
[37] R. Coehoorn and R. A. de Groot, J. Phys. F: Met. Phys. **15**, 2135 (1985).